

Contact forces at the sliding interface: Mixed versus pure model alkane monolayers

Paul T. Mikulski,^{a)} Guangtu Gao, Ginger M. Chateaufneuf, and Judith A. Harrison
Departments of Physics and Chemistry, United States Naval Academy, Annapolis, Maryland 21403

(Received 30 July 2004; accepted 12 October 2004; published online 17 December 2004)

Classical molecular dynamics simulations of an amorphous carbon tip sliding against monolayers of *n*-alkane chains are presented. The tribological behavior of tightly packed, pure monolayers composed of chains containing 14 carbon atoms is compared to mixed monolayers that randomly combine equal amounts of 12- and 16-carbon-atom chains. When sliding in the direction of chain cant under repulsive (positive) loads, pure monolayers consistently show lower friction than mixed monolayers. The distribution of contact forces between individual monolayer chain groups and the tip shows pure and mixed monolayers resist tip motion similarly. In contrast, the contact forces “pushing” the tip along differ in the two monolayers. The pure monolayers exhibit a high level of symmetry between resisting and pushing forces which results in a lower net friction. Both systems exhibit a marked friction anisotropy. The contact force distribution changes dramatically as a result of the change in sliding direction, resulting in an increase in friction. Upon continued sliding in the direction perpendicular to chain cant, both types of monolayers are often capable of transitioning to a state where the chains are primarily oriented with the cant along the sliding direction. A large change in the distribution of contact forces and a reduction in friction accompany this transition. © 2005 American Institute of Physics. [DOI: 10.1063/1.1828035]

I. INTRODUCTION

Self-assembled monolayers (SAMs) are promising candidates as boundary layer lubricants for use in nanoscale devices.¹ Because these monolayers are composed of molecularly thin, densely packed organic moieties on solid substrates, they represent ideal model systems for the study of lubrication at the molecular level.² As a result, the frictional properties of SAMs have been studied extensively using atomic-force microscopy (AFM).^{2–30} The effects of chain length, packing density (order), and terminal group on friction are some of the variables that have been examined. Perry and co-workers used AFM to examine the friction of SAMs composed of spiroalkanedithiols.^{2,7,11} The use of this type of molecule allows the effects of crystalline order at the sliding interface on friction to be unambiguously probed. The spiroalkanedithiol molecules attach to the substrate and then branch into two chains. Systematically shortening one of the chains caused a progressive increase in disorder and an increase in friction. The effect of having longer chains mixed with shorter chains on friction was also examined by Salmeron and co-workers.⁴ In that work, the islands of alkanethiols composed of chains of two lengths had higher friction at a given load than the islands composed of chains of a single length. In addition, the two component islands demonstrated a different friction versus load response at low loads than the one component islands.

There have been a number of studies that have examined the structural and tribological properties of SAMs using molecular dynamics (MD) simulations.^{31–52} Motivated by the experimental work that examines the friction of mixed chain-

length SAMs, we have used MD to investigate monolayers of *n*-alkane SAMs composed of chains of a single length (pure) and those composed of chains of two lengths (mixed). The chains are chemically bound to a diamond substrate and an amorphous hydrocarbon tip is used to probe friction between the monolayers and the tip. This study focuses on the contact forces between the tip and the chain groups within the monolayers. The friction difference between the pure and mixed monolayers is elucidated by examining the distribution of contact forces during sliding. Insight into friction anisotropy in these systems is also gained from an examination of the contact forces. The focus on individual chain groups gives insight to the nature of forces exerted on the tip over length scales of only a few angstroms, and thus provides a window into fundamental processes that is currently unavailable experimentally.

II. SIMULATION DETAILS

As in earlier studies of SAMs by Harrison and co-workers,^{31,35,36,41,53–55} this study uses the adaptive intermolecular reactive empirical bond-order potential (AIREBO).⁵⁶ This potential was parametrized to model hydrocarbon systems of all phases. Like the REBO^{57–59} potential from which it is derived, the AIREBO potential is capable of modeling chemical reactions. Thus, the formation and creation of bonds that can accompany compression and sliding are possible in these simulations. Unlike the REBO, the AIREBO potential includes long-range interactions between nonbonded atoms. While for most atomic pairs in the system it is very clear whether the atoms are bonded or not, during a chemical reaction atomic pairs can arise for which the bonding characteristics are not clear. The strength of the

^{a)}Electronic mail: mikulski@usna.edu

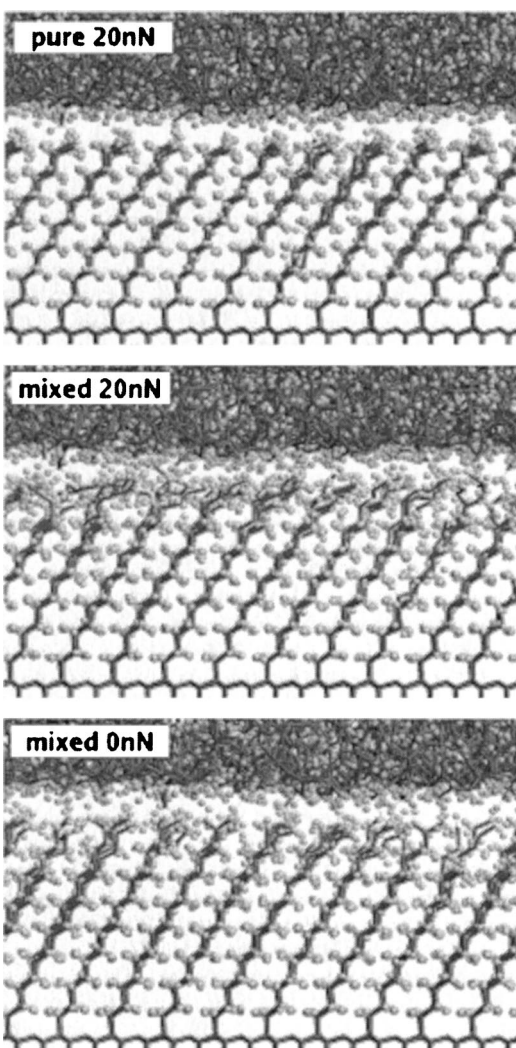


FIG. 1. Snapshots of some of the model systems under investigation. Carbon bonds are shown in thick wireframe, hydrogen atoms are shown as gray spheres. The pure SAM is composed of 100 chains each with 14 carbon atoms anchored in a 2×2 arrangement to a diamond (111) substrate. The mixed SAM is similarly constructed with a 1:1 ratio of 12 and 16 carbon-atom chains randomly mixed. The top two snapshots show the pure and mixed monolayers under loads of 20 nN (0.90 GPa). The bottom snapshot shows the mixed monolayer at a load of 0 nN.

AIREBO potential is that it smoothly interpolates between the bound and unbound states in a self-consistent manner. This is accomplished by modifying simple pairwise interactions according to the local chemical environment of each pair.

Each model SAM is composed of 100 linear hydrocarbon (*n*-alkane) chains covalently bonded in a 2×2 arrangement to a diamond (111) substrate (Fig. 1). Recent simulations that examined the friction of alkylsilane monolayers showed that system dynamics were independent of system size, for systems between 100 and 1600 chains.³³ Periodic boundary conditions of ≈ 50 and 44 \AA are imposed in the plane containing the monolayer (*xy* plane). The diamond substrate is composed of three layers of carbon atoms each containing 400 atoms. Each chain of the pure SAM has the formula $-(\text{CH}_2)_{13}-\text{CH}_3$. The mixed SAM contains equal amounts of 12 carbon-atom chains $-(\text{CH}_2)_{11}-\text{CH}_3$ and 16

carbon-atom chains $-(\text{CH}_2)_{15}-\text{CH}_3$, which are randomly mixed. This two-component mixture results in a monolayer with the same total number of carbon and hydrogen atoms as in the pure monolayer. Thus, both systems examined here (substrate plus SAM) contain a total of 5500 atoms; this ensures that any tribological differences between the pure and mixed systems are not associated with a differing number of atoms or monolayer mass. The samples were equilibrated prior to combining with the model tip. Equilibration reveals a highly ordered structure with chains canted predominantly in the *yz* plane (Fig. 1) and leaning in the positive *y* direction as seen in previous simulations.^{31,35,36,41,53-55}

The ability of the AIRBEO potential to model the breaking and forming of bonds was important in the construction of the model tip. In this work, the tip, or counterface, was constructed from amorphous carbon because a number of groups that perform AFM experiments of friction are beginning to use diamondlike carbon coated tips,⁶⁰ and because it is not commensurate with the monolayer. Several techniques for generating amorphous carbon samples have been described in the literature.⁶¹⁻⁷¹ The most computationally feasible technique is the quenching of liquid carbon. While this method is simple and effective, it is difficult to generate amorphous carbon films with different structures or with suitable surface structures.^{61,64} Because we are interested in generating samples that have properties similar to those obtained experimentally, and with a surface structure where all bonds are saturated, adaptations have been made to the quenching techniques described in the literature. Saturating all the bonds on the surface of the tip ensures that adhesion between the tip and the monolayer will not occur⁶⁴ so that wearless friction can be unambiguously examined.

A high-temperature liquid hydrocarbon mixture is generated by equilibrating a random distribution of carbon and hydrogen atoms at 10 000 K. The periodic boundary conditions in the *xy* plane match those of the model SAMs. To provide an environment that encourages the formation of a fairly flat surface with hydrogen termination, the carbon atoms were confined to a smaller length in the *z* dimension than the *z* periodic boundary conditions during equilibration. This mixture was quenched over a picosecond time interval because this is the time scale associated with the cooling of thermal spikes following ion deposition in the growth of amorphous carbon structures.⁶³ The sample was then equilibrated at room temperature with periodic boundary conditions in only the *xy* plane. The resulting tip density is $\approx 2.3 \text{ g/cm}^3$ and 35% of the tip atoms are hydrogen. These specifications fall within the wide range of specifications that characterize diamondlike carbon.⁷² A nominally flat surface is desired because typical AFM tips have radii of curvature of the order of hundreds of angstroms, whereas the model systems under investigation here are only of dimensions 50 by 44 \AA (a size that is computationally feasible). The surface contained a few unsaturated carbon atoms and exhibited a number of complex and a few unphysical features; consequently, the structure was trimmed back and some carbon atoms were hydrogen terminated. Following these modifications, the tip was further equilibrated. The resulting surface of the tip exhibits a mild level of roughness and a high level

of chemical saturation. The full amorphous structure was sliced at a plane of constant height in the z direction such that the tip used in the simulations contains 5500 atoms. Slicing severs many chemical bonds at the top of the tip. Therefore, of the remaining tip atoms, the top 1500 atoms are held rigid relative to one another to insure that the lowest rigid atoms that are directly bound to free atoms have all bonds still intact.

The key feature of the model tip is the lack of periodic structure beyond the periodic boundary conditions of the system. A distinguishing feature that differentiates the pure monolayers compared to the mixed monolayers is their ordered structure at the tip-monolayer interface when under a substantial load (both monolayers show ordered structure in the lowest 12 chain groups). The use of an amorphous tip ensures that any difference in friction between pure and mixed monolayers is not due to a commensurate geometry between tip and sample.

Sliding is accomplished by moving the rigid atoms of the tip at a constant speed of approximately 0.22 \AA/ps along the sliding direction. This speed is typical for MD simulations of this scale due to computational limitations^{31–33,35,36,41,53–55} but orders of magnitude larger than experimental sliding speeds.^{4,11,23,25,26,72,73} Grest and co-workers have undertaken a study of the effect of sliding speed in alkylsilane monolayers and have shown that system dynamics were similar using relative speeds of 0.2, 2, and 20 m/s between two monolayers in sliding contact.^{32,33} Perry and Harrison also found that the friction between contacting diamond (100) surfaces was independent of sliding speed.⁷⁴ In hydrocarbon systems, the simulation time step is governed by the fastest process modeled, or the vibration of hydrogen atoms. The adopted time step of 0.20 fs means that two passes over the sample requires two million simulation steps and corresponds to a modeled sliding time of 400 ps and a sliding distance of 88 Å. Berendsen thermostats set at 290 K were applied separately to the tip and sample to dissipate the heat generated by sliding.^{75,76} The results reported here are insensitive to the type of thermostat used.

The sliding simulations reported here were conducted at a constant target load. The load on the tip was maintained with a simple feedback loop. At each step, the net vertical force (load) exerted on all the tip atoms was calculated. If the load calculated in this way did not equal the target load, all the tip atoms were either raised or lowered by an amount δz , where $\delta z = 0.1 \delta y$. The quantity δy is the fixed distance the rigid atoms of the tip are moved along the sliding direction at each simulation step ($\delta y \approx 4.4 \text{ fm}$). While the load calculated using rigid tip atoms correlates very strongly with the load calculated using all tip atoms, summing over only rigid atoms introduces a much higher level of variation over intervals of only a few simulation steps compared to summing over all tip atoms. Using all tip atoms renders the feedback loop insensitive to the large variation in forces between the rigid tip atoms and the free tip atoms to which they are directly bonded. The degree to which the vertical motion of the tip responds to changes that occur over single simulation steps is also minimized by fixing this motion to be only 10%

of the forward tip motion at a given simulation step. Of the two million simulation steps in a given sliding simulation, only 1.2% of these steps are steps where the tip changes direction.

Contact pressures in AFM experiments typically range from 0.1 to several gigapascals. Except for terminal groups, alkyl chains of alkanethiols⁸ and alkylsilanes⁷⁷ retain their well-ordered close-packed structure in this pressure range. At much higher localized pressures, it is possible to use an AFM tip to laterally displace SAM molecules and disrupt their ordered structure on the substrate surface.⁷⁸ The target load of 20 nN examined in these simulations corresponds to a pressure of 0.90 GPa and thus falls conservatively within the range routinely probed by AFM experiments where SAMs maintain their ordered structure.²³ In a computational study of the higher pressures where lateral displacement of SAM molecules on the substrate has been observed experimentally, it may be important to address carefully how the bonding of head groups to the substrate surface is modeled.

Initial simulation configurations were created by placing the tip over the monolayers in positions that minimized the initial potential energy. Four such configurations, that differed in the position of the tip in the xy plane, were constructed for each monolayer. These eight systems were then equilibrated while sliding along the direction of chain cant (to the right in Fig. 1) and adjusting to the target load. A projection of the chain backbones, moving from the bottom of the chain to the top, in the xy plane points predominantly in the positive y direction. Several target loads were examined. In this work, results for a target load 20 nN are the primary focus with some commentary on 0 nN target load results. Once the systems showed steady-state dynamics and sliding conducted past a full length of the sample, sliding was continued and friction data were collected for two full passes across the sample.

III. RESULTS

A. Net friction

Snapshots of pure-monolayer and mixed-monolayer systems under 20 nN of load and of the mixed-monolayer system under 0 nN of load are shown in Fig. 1. At the sliding interface, the mixed system is disordered under repulsive loads because the ends of the randomly attached long chains (16 carbon atoms) have collapsed to fill the vacant volumes over the short chains (12 carbon atoms). Because all chains in the mixed system have at least 12 carbon atoms in the chain backbone, the lower 12 chain groups in the mixed monolayers show the same uniform cant and ordered structure that is evident in the pure monolayers where all chains are of the same length (14 carbon atoms). At 0 nN of load, the long chains of the mixed systems are stretched out, taking on a uniform cant that extends over the full length of all chains. Thus, the volume above the short chains is unfilled. The application of load to the pure monolayer increases the cant of all the chains without introducing disorder at the sliding interface. This effect was also observed when a hydrogen-terminated diamond (111) surface was used to compress the monolayers.^{35,36,41}

TABLE I. Friction and load results for the pure and mixed systems. Four independent slides (labeled *A*, *B*, *C*, and *D*) were conducted for each monolayer type. The average force between each monolayer chain group ($-\text{CH}_2-$ or $-\text{CH}_3$) and the tip is calculated every 2000 simulation steps (0.083 Å of sliding). Positive and negative contributions to each component of the net force between the sample and the tip are tracked separately by noting the sign of each force component for each chain group over each 2000 simulation step window. Positive and negative contributions to the friction and load are indicated in normal type while the net friction and load are indicated in bold.

System	Friction (nN)	Load (nN)
Pure <i>A</i>	5.56–4.78= 0.79	27.41–7.33= 20.08
Pure <i>B</i>	5.55–4.63= 0.92	27.37–7.30= 20.07
Pure <i>C</i>	5.57–4.69= 0.88	27.40–7.33= 20.06
Pure <i>D</i>	5.56–4.73= 0.83	27.37–7.30= 20.07
Mixed <i>A</i>	5.15–3.29= 1.86	25.07–5.01= 20.06
Mixed <i>B</i>	5.15–3.20= 1.95	25.03–4.92= 20.11
Mixed <i>C</i>	5.14–3.33= 1.81	25.05–4.98= 20.07
Mixed <i>D</i>	5.16–3.26= 1.90	25.06–5.01= 20.05

Taking the sliding direction as positive, the definition of friction that is most closely connected with the quantity that is measured experimentally is the size of the average net force on the rigid atoms of the tip along the sliding direction. A comparison of the friction calculated using this definition against a calculation of the net force along the sliding direction on all atoms in the sample shows that both give the same result to within less than a percent for all systems under investigation here. Furthermore, though the instantaneous force on rigid tip atoms can show much larger rapid variation than the instantaneous force on all sample atoms, these quantities are very highly correlated. In the following discussion, focus is placed on the forces on all sample atoms because there are a number of ways in which these forces can be analyzed to gain insight into system dynamics at the sliding interface.

The friction and load calculated from two passes over the sample are shown in Table I for all simulation systems at a target load of 20 nN. The net friction and load are shown in bold. The pure systems consistently exhibit less than half of the friction found in the mixed systems. This is a general feature of these systems when the loads are substantial enough to collapse the ends of the long chains in the mixed system (loads of a few nanonewtons up to at least 30 nN or 1.4 GPa) and when sliding along the direction of chain cant. It should also be noted that the same results are obtained using a variety of load management methods, such as adjusting tip height by using stronger feed back loops ($\delta z = 0.3\delta y$ and $\delta z = \delta y$) or by choosing a fixed height slide.

At attractive loads (a few nanonewtons below 0 nN) and at 0 nN, the contact area is significantly different in these two systems and this has a substantial effect on the overall friction. In this load regime, friction per chain group in strong contact with the tip exhibits the same dramatic difference between pure and mixed systems that is observed at positive loads. However, in the mixed system only the long chains, or half as many chains as in the pure system, are in contact with the tip at 0 nN. The load of 0 nN is achieved by a balance of attractive and repulsive forces with the net repulsive force

scaling approximately with the number of chains in direct contact with the tip. With twice the number of chains at half the friction per chain, the net friction in pure systems is comparable to that in mixed systems at 0 nN ($0.34\text{ nN} \pm 0.02$ and $0.38\text{ nN} \pm 0.03$ for the pure and mixed systems, respectively).

B. Contact forces

In an effort to gain insight into the differences in friction between pure and mixed monolayers, contact forces between the tip and monolayer chain groups were examined. A chain group is composed of a $-\text{CH}_2-$ or a $-\text{CH}_3$ entity. The contact force on a single chain group is defined as

$$\mathbf{F} = \frac{1}{N} \sum_i^N \left(\sum_j^{\text{tip}} \sum_k^{\text{group}} \mathbf{F}_{jk} \right), \quad (1)$$

where i is the sum over 2000 simulations steps (N), j sums over the 5500 tip atoms, k sums over a given single carbon atom of the SAM and its attached hydrogen atoms (chain group), and \mathbf{F}_{jk} is the instantaneous force between atoms j and k . Two passes of the tip over the sample corresponds to 2×10^6 million simulation steps. Thus, the contact force is calculated 1000 times for each chain group and is averaged over 2000 steps. Averaging forces over 2000 simulations steps corresponds to 0.083 Å of sliding, or 1/500 of the length of the sample. This time-averaging window is small enough to track atomic-scale dynamics and large enough to average out thermal fluctuations.

The contact force along the sliding direction of each chain group can be characterized as either resisting the motion of the tip (positive force) or pushing the tip in the sliding direction (negative force). In the same way, each chain group is characterized as either being in repulsive contact (positive force) or attractive contact (negative force) with the tip. Significant insights can be obtained by separating these positive and negative contributions to the friction and the load and summing over all chain groups in the sample. Table I shows the average contact forces for both the pure and the mixed systems when sliding along the direction of chain cant. The same net forces can also be obtained by summing the net force on each sample atom due to interactions with all atoms in the system and averaging over the run. However, the separation of these net forces into positive and negative contributions from interactions between chain groups and the tip relies on the definition of contact force given above.

The magnitudes of the positive and negative forces in all the pure systems exceed those found in all mixed systems without exception. This is also true of the transverse component of the contact force (the component in the plane containing the monolayer but transverse to the sliding direction). The average separation between the rigid layers of the tip and sample is $0.91\text{--}0.94$ Å larger in any given mixed system than it is in any pure system. Thus, the ordered, and slightly flatter, surface of the pure systems brings more atoms near to the tip. This results in larger attractive forces and requires larger repulsive forces to maintain the 20 nN target load. The slightly-flatter structure of the pure systems does not inhibit the generation of force components in the sliding plane to

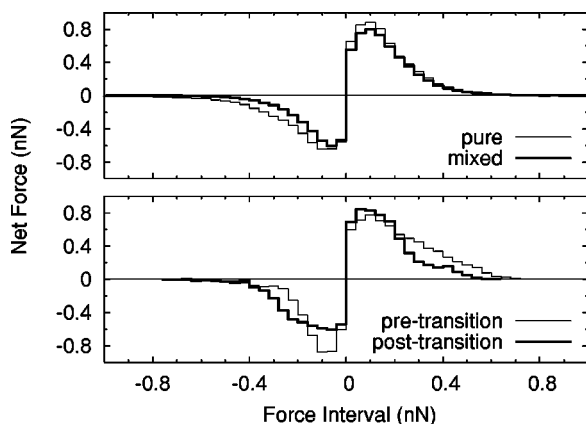


FIG. 2. The distribution of contact forces along the sliding direction. The force between each chain group ($-\text{CH}_2-$ or $-\text{CH}_3$) and the tip is binned over intervals of 2000 simulation steps for the top 200 chain groups of each monolayer (the top two chain groups of each chain in pure SAMs and the top four chain groups of each long chain in mixed SAMs). Positive force intervals correspond to chain groups resisting tip motion, while negative force intervals indicate chain groups pushing the tip along. Friction can be calculated by summing all bins. The top figure compares pure and mixed monolayers when sliding in the y direction (to the right in Fig. 1). All four runs (A , B , C , and D) are binned together for each monolayer type. The bottom figure looks at a single pure monolayer (run C) after sliding has been switched from the y direction to the x direction. After sliding over a significant length of the sample, the chains within this pure monolayer rotated so that they were more aligned with the new sliding direction. The histogram compares the force distribution before and after the rotation of the chains.

achieve low friction. Rather, the pure systems are characterized by either larger, and/or more frequent, interactions between tip and sample along the sliding direction. Therefore, pure systems exhibit lower friction not because the scale of forces is smaller, but because there is significantly less difference between forces that resist tip motion (positive contributions to the friction) and forces that push the tip along (negative contributions to the friction).

Only those chain groups close to the sliding interface generate appreciable contact forces. In the pure monolayers at the target load of 20 nN, the 200 groups closest to the interface are the top two groups from each of the 100 chains, while the top 200 SAM groups in the mixed monolayers are the top four groups of each of the 50 long chains. The lowest 12 groups of each chain in all systems are excluded with less than 1% effect on the net friction and less than 2% effect on the positive and negative contributions to the friction.

The individual contact forces on the top 200 groups of each SAM can be plotted as a histogram. Figure 2 (upper panel) shows the distribution of contact forces in the sliding direction for both the pure and the mixed systems with the four independent runs binned together. In this figure, the dependent variable is the summed net force in each force interval (friction is thus the sum of all bins) rather than a count. Forces that resist the motion of the tip are positive and those that “push” the tip in the sliding direction are negative. The shape of the distributions containing the positive forces is similar for the pure and mixed systems. Thus, the pure and mixed systems resist the motion of the tip in similar fashions though the pure systems exhibit a higher frequency of small resistive interactions, which is apparent from the noticeably

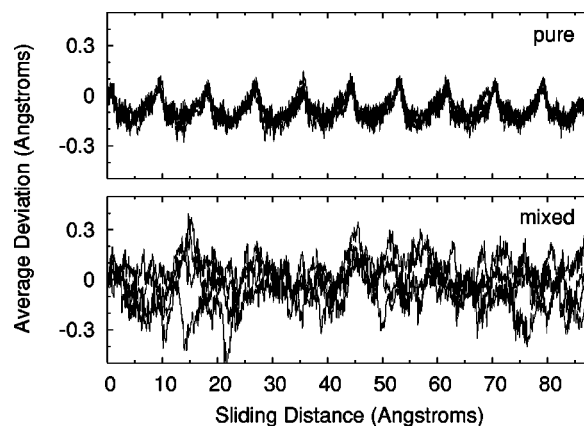


FIG. 3. Average deviation along the sliding direction of the top 200 monolayer chain groups relative to their starting positions for both the pure and mixed systems. Sliding is in the y direction (to the right in Fig. 1).

larger resistance to tip motion in the smaller, positive force intervals. In contrast, the negative contact forces (forces that push the tip along) of the pure and mixed systems are markedly different. This suggests that the ordered structure of the pure systems is conducive to returning the energy stored during resistive processes as mechanical energy, while the disordered, slightly less dense, structure of the mixed systems at the sliding interface results in the conversion of the stored potential energy into thermal energy. The resistive forces at medium to high force intervals indicates that the scale of forces is similar in the pure and mixed systems. While the larger forces in the pure systems at small positive force intervals indicate a more densely packed structure that brings more chain groups in more frequent contact with the tip. With its densely packed structure, the pure monolayer chain groups exhibit a much higher level of symmetry between positive and negative forces along the sliding direction.

The coordinated response of chains in the pure systems during sliding aides in the recovery of mechanical energy. The average deviation along the sliding direction of the top 200 chain groups relative to their starting positions is shown in Fig. 3. The position of a chain group ($-\text{CH}_2-$ or $-\text{CH}_3$) is taken to be the average position of the group’s carbon atom averaged over 2000 simulation steps. It is clear from examination of these data that chains in the pure system respond in a correlated manner to the motion of the tip, and maintain the periodicity of their arrangement on the substrate despite the fact that the tip is amorphous. This type of coordinated motion has been observed in previous simulations where flat, periodic tips have been used.^{35,36,41} In contrast, the groups in the mixed system do not reflect the underlying order of the lower groups of the monolayers or the substrate. The positions of chain groups in the mixed system vary over a much wider range than the groups of the pure system. This is confirmed by a calculation of the standard deviation of position along the sliding direction for each chain group averaged over the top 200 chain groups. Mixed systems give an average standard deviation of 0.58 Å whereas pure systems give an average deviation of only 0.25 Å. Earlier studies conducted by our group have also found this correlation between restricted range of motion and lower friction.³⁵

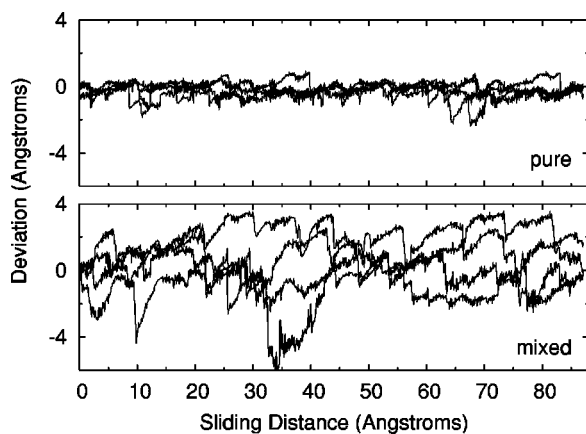


FIG. 4. Characteristic trajectories of individual chain groups from pure (upper panel) and mixed (lower panel) monolayers while sliding in the y direction. The deviation is the change in position along the sliding direction relative to the chain group's starting position (position is taken to be the average position of the chain group's carbon atom over 2000 simulation steps). The four trajectories chosen for each monolayer type are the four chain groups from the set of runs (A , B , C , and D) that generate the largest net contact force along the sliding direction.

A detailed examination of the motion of the individual chain groups reveals a variety of characteristic motions. Figure 4 shows the position along the sliding direction of a few representative trajectories for each system. These trajectories are the four chain groups of the four sliding systems that give the largest average contact force along the sliding direction. The trajectories of chain groups from the mixed systems typically show a wider range of movement by way of larger movements around a general area and dramatic rapid transitions from one general area to another. The general differences between the pure and mixed systems are dramatically characterized by these trajectories; however, they fail to convey that, though few in number, there can be chain groups in the pure systems that show movement more typically associated with chain groups from the mixed systems and vice versa.

C. Sliding direction

After steady-state sliding along the y direction (predominate direction of chain cant) was established, the sliding direction was changed to the x direction in all eight systems. Analyses of the distribution of contact forces and the average deviation of the position of the chain groups from their initial positions were also done for these slides. At the beginning of the slides, the cant of chain backbones is nearly perpendicular to the sliding direction. Examination of the average deviation of the position of the chain groups (Fig. 5) in the mixed systems shows that all mixed systems undergo a transition corresponding to a rotation of the chains within the monolayer in the horizontal plane. A signature of such a transition is the increase in the average x position deviation from near zero to large positive values around 7 Å. After the transition, the cant of the reoriented chains is more closely aligned with the sliding direction. In contrast, only two of the pure systems successfully transition after 88 Å of sliding,

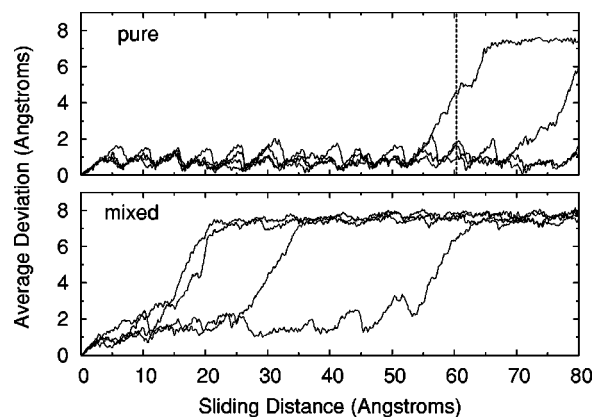


FIG. 5. Average deviation along the sliding direction of the top 200 mono-layer chain groups relative to their starting positions. The sliding direction is in the x direction (out of the page in Fig. 1) with the chains initially canted along the y direction. The steep rise over about 7 Å evident in most systems corresponds to a change in the azimuthal angle of the monolayer chains so that they are more closely aligned with the sliding direction. All four of the mixed monolayer runs (lower panel) A , B , C , and D undergo a transition. The dashed vertical line in the upper panel (pure system) represents the position of a transition from high friction (2.45 nN) to low friction (1.21 nN) in the first system to transition.

though it is possible that the untransitioned pure systems would undergo a change in chain cant upon continued sliding.

Further insight into the reorientation of the monolayer to a new orientation can be gleaned from an examination of the azimuthal angles of the individual chains. The azimuthal angle is defined in the following way. Consider the x and y components of the vector from carbon atom 1 (closest to the substrate) to carbon atom 11 inside each chain (chain vector). The azimuthal angle is taken to be the inverse tangent of y/x . Thus, the azimuthal angle is the angle between the x direction and the projection of the chain vector constructed from carbon atoms 1 to 11. The azimuthal angle for all 100 chains is plotted as a function of sliding distance for the pure system that transitions after 60 Å of sliding in the x direction (Fig. 6). At the start of the sliding, the angle is close to 90° indicating that the chains are primarily canted in the y direction. As sliding progresses, the chains within the monolayer

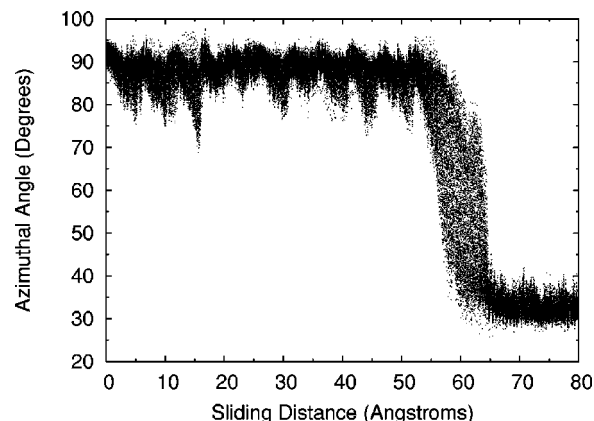


FIG. 6. Azimuthal angle, the angle between chain backbones projected into the xy plane and the sliding direction, as a function of sliding distance for the first pure system to transition by way of rotation of the entire monolayer.

make several attempts to transition. This is apparent from the periodic downward spikes in the angles extending down to 70° – 75° . After ≈ 52.5 Å of sliding, the chains within the monolayer begin to reorient. The angles of the individual chains begin to decrease. After ≈ 65 Å of sliding, the reorientation of the chains is complete and all the chains have azimuthal angles slightly larger than 30° . Thus, the chains have passed over a potential energy barrier between two crystallographically equivalent directions of the underlying diamond substrate. The azimuthal angle as a function of sliding distance shows the same general behavior in the mixed system. Note that in the intermediate region of the transition there is a spread in chain angles that is over 40° wide. Thus the transition does not occur in complete unison across all chains in the monolayer, though all chains do respond within a few angstroms of sliding.

Both the mixed and the pure systems exhibit higher friction when sliding in the x direction compared to the y direction. Friction in the pure systems shows a dramatic increase of over a factor of 2 with the change in sliding direction. The new sliding direction does not “see” the same periodicity as the original sliding direction (recall the differing periodic boundary conditions in the x and y directions) due to the structure of the underlying diamond (111) substrate. Consequently, the orientation and organization of chains relative to the x sliding direction in the pure monolayer after the reorientation are different than they were in the analogous y direction slides. Thus, while the friction does decrease after the reorientation (transition), it is still higher in both systems than in the original y direction slides where chains were aligned along the sliding direction and were aligned favorably with respect to the crystal structure of the underlying substrate.

Focusing on the first pure system that transitions, the vertical line near 60 Å of sliding in Fig. 5 indicates the region where a transition from high friction to low friction occurs. The size of the fluctuations in the average deviation data are larger before the transition compared than after the transition. In addition, the average standard deviation of chain group position along the sliding direction for the untransitioned pure systems is 0.46 Å compared to the 0.25 Å for the pure systems when sliding in the y direction. Both of these comparisons show the correlation between restricted range of motion and low friction. Histograms of contact forces for the first pure system to transition were constructed by separating the pretransition and posttransition phases. It is clear that the shape of the positive and negative force distributions have changed as a result of the transition: the scale of forces (the size of forces in the medium to high positive force intervals) is significantly less, and the negative force distribution shows a more even distribution across negative force intervals. With regard to sliding direction, it is the scale of resistive forces that is primarily responsible for the observed friction anisotropy; whereas, in the comparison above between mixed and pure monolayers, it was the degree of symmetry between resistive forces and “pushing” forces that explained the observed frictional differences. Some of the

mixed systems also show a change in contact-force-distribution shape after the systems transition. However, this effect is not as pronounced as it is in the pure systems.

IV. DISCUSSION

A number of groups have used AFM to examine the friction of alkanethiol^{2,4,7,11,12,23,26,30,79} and alkylsilane SAMs.⁸⁰ These experimental studies show that as the length of the alkanethiol chain increases, the friction decreases. However, it has also been shown that as the chain length increases so does the packing density.⁸¹ Thus, it seems that increasing the packing density of the chains, and thereby increasing order within the monolayer, decreases friction. Perry and co-workers used spiroalkanedithiol-based SAMs to unambiguously examine the effect of order on friction.^{2,7,11} In these studies, the packing density at the point where the chains attached to the substrate was fixed. Because two chains originate from each attachment point, varying the length of one of these chains alters the order at the sliding interface. Various surface science techniques were used to confirm that shortening one of the chains led to more disorder at the surface of the monolayer. The more disordered systems had higher friction. Salmeron and co-workers examined islands of alkanethiols composed of only 12 or 16 carbon atoms and islands containing a mixture of 12 and 16 carbon-atom chains. The measured friction of the mixed-chain system was always higher than the islands with chains of one length. In addition, the response of friction to load was different in the mixed than in the pure islands under low loads. Thus, the correlation between crystalline order and nanoscale frictional properties is well established.

In a unique study, van de Vegte *et al.* examined the tribological behavior of opposing surfaces of unsymmetrical dialkyl sulfides on Au with varying chain lengths using a scanning force microscope.¹² These molecules are also composed of two chains and one attachment point to the substrate. In this work, both the tip and the substrate were covered with monolayers. The tip was covered with chains composed of a mixture of 10 and 18 carbon atoms. The lengths of one of the chains in the substrate was systematically varied and the friction measured. As the difference between the chain lengths increased so did the friction and the friction coefficients. In this case, the authors attribute the friction differences to increased interdigitation of the chains between the tip and the monolayer.

Two compatible hypothesis have been put forth to explain the correlation between friction and order. Salmeron and co-workers suggested that it is easy to deform the protruding ends of the molecules.⁴ The increased number of deformation modes leads to increased energy dissipation and the higher friction. Perry and co-workers argue that the loosely packed chains undergo enhanced van der Waals contact with the AFM tip, which gives rise to enhanced frictional responses during sliding. In other words, the number of atomic contacts falling within a given area of contact is greater for liquidlike films (disordered) than for crystalline films.^{2,11}

The molecular dynamics simulations reported here were aimed at elucidating the connections between order and fric-

tion. The friction of SAMs composed of 14-carbon-atom chains (pure systems) and those composed of a random mixture of equal amounts of 12- and 16-carbon-atom chains (mixed systems) was examined. When sliding along the direction of chain cant under repulsive loads, pure SAMs consistently exhibit less than half the net friction of mixed SAMs. The origin of this friction difference was elucidated by examining the contact forces between the tip and the individual groups in the chains that compose the SAMs. Examination of the contact forces allows for lateral force to be separated into components that resist sliding (positive forces) and those that push the tip in the sliding direction (negative forces). Thus, the net friction is obtained by summing the positive and negative contributions to sliding. Though pure SAMs show a higher frequency of interactions between chain groups and the tip (due to the uniform chain length), they possess a high level of symmetry between forces that resist the motion of the tip and forces that push the tip along. It is this symmetry between positive and negative forces along the sliding direction, rather than the overall scale of forces or the strength of resistive forces, that is responsible for the low friction of the pure monolayers. In other words, the ordered, densely packed nature of the pure monolayers allows the energy stored when the monolayer is resisting tip motion (positive forces) to be retained as mechanical energy when the monolayer pushes on the tip (negative forces). The shape of the distribution of negative contact forces in the mixed monolayers is different from the shape of the positive distribution. Thus, mechanical energy is not efficiently retained as the tip passes over the chains. The increased range of motion of the protruding tails of the chains allows for the dissipation of energy.

It should also be noted that under repulsive loads, the protruding chains in the mixed systems are pushed down creating disorder at the sliding interface. As a result, the last four groups in the long chains contribute to the contact forces between the tip and the monolayer. In the pure system, only the top two chain groups contribute to the contact forces. Because there is an equal mixture of long and short chains in the mixed systems, the number of chain groups in contact with the tip is equal to the number in the pure system under repulsive loads. However, it should be noted that there are cases when the number of groups in contact with the tip would not be equal. The most obvious case where this would be true is if the ratio of long to short chains was not equal. For example, if the number of long chains was slightly larger than the number of short chains, the number of chain groups in contact with tip would be larger in the mixed system. The difference in lengths between the long and short chains should also influence the contact area under repulsive loads. In contrast, under attractive, or 0 nN, loads only the top two groups of the protruding chains in the mixed system contribute to the contact forces. Thus, the number of contacting chain groups is half what it is in the pure systems. Thus, the reduction in contact area at 0 nN is responsible for the mixed and pure systems having very nearly the same net friction.

Our previous MD studies of the friction of *n*-alkane chains on diamond utilized a hydrogen-terminated diamond (111) surface as a tip.^{35,36,41} In an effort to remove any ef-

fects of commensurability between the tip and the SAM, an amorphous carbon tip was used for the studies reported here. The use of an amorphous tip clearly shows that at least under the specialized circumstance of sliding in the direction of chain cant, there are notable differences resulting in lower net friction under repulsive loads for pure SAMs contrasted with mixed SAMs.

The ordered densely-packed structure at the sliding interface is a necessary, but not a sufficient condition for yielding low friction. Specifically, if the sliding direction is changed to one that is transverse to the cant of the chains the friction increases. For example, the high level of symmetry evident in the force distributions of both systems is lost due to both an increase in resisting forces and a decrease in pushing forces when the sliding direction is changed. However, under continued sliding in the direction perpendicular to chain cant, SAMs are capable of reorienting by way of a rotation of the monolayer chains such that the symmetry between positive and negative forces along the sliding direction is at least partially regained. While reoriented pure SAMs show a lower friction than reoriented mixed SAMs, pure SAMs are less likely to make the transition (only two of the four pure SAMs transitioned after approximately two passes of the tip across the sample). The conditions that result in the reorientation of SAMs are currently under investigation.

ACKNOWLEDGMENTS

This work was supported by the Naval Academy (NARC program), ONR (Contract No. N00014-04-20212), and AFOSR (Contract No. NMIPR045203577). J.A.H. thanks M. Salmeron and S. S. Perry for many helpful discussions.

- ¹A. Ulman, *Chem. Rev. (Washington, D.C.) (Washington, D.C.)* **96**, 1533 (1996).
- ²S. Lee, Y. S. Shon, R. Colorado, R. L. Guenard, T. R. Lee, and S. S. Perry, *Langmuir* **16**, 2220 (2000).
- ³N. M. Brewer and G. J. Leggett, *Langmuir* **20**, 4109 (2004).
- ⁴E. Barrena, C. Ocal, and M. Salmeron, *Surf. Sci.* **482–485**, 1216 (2001).
- ⁵N. M. Brewer, B. D. Beake, and G. J. Leggett, *Langmuir* **17**, 1970 (2001).
- ⁶S. Lee, A. Puck, M. Graupe, R. Colorado, Y.-S. Shon, T. R. Lee, and S. S. Perry, *Langmuir* **17**, 7364 (2001).
- ⁷S. S. Perry, S. Lee, Y.-S. Shon, R. Colorado, and T. R. Lee, *Tribol. Lett.* **10**, 81 (2001).
- ⁸M. Salmeron, *Tribol. Lett.* **10**, 69 (2001).
- ⁹E. Barrena, C. Ocal, and M. Salmeron, *J. Chem. Phys.* **113**, 2413 (2000).
- ¹⁰B. D. Beake and G. J. Leggett, *Langmuir* **16**, 735 (2000).
- ¹¹Y.-S. Shon, S. Lee, R. Colorado, S. S. Perry, and T. R. Lee, *J. Am. Chem. Soc.* **122**, 7556 (2000).
- ¹²E. W. van der Vegte, A. Subbotin, G. Hadziioannou, P. R. Ashton, and J. A. Preece, *Langmuir* **16**, 3249 (2000).
- ¹³E. Barrena, S. Kopta, D. F. Ogletree, D. H. Charych, and M. Salmeron, *Phys. Rev. Lett.* **82**, 2880 (1999).
- ¹⁴E. Barrena, C. Ocal, and M. Salmeron, *J. Chem. Phys.* **111**, 9797 (1999).
- ¹⁵B. D. Beake and G. J. Leggett, *Phys. Chem. Chem. Phys.* **1**, 3345 (1999).
- ¹⁶A. R. Burns, J. E. Houston, R. W. Carpick, and T. A. Michalske, *Phys. Rev. Lett.* **82**, 1181 (1999).
- ¹⁷R. W. Carpick, D. Y. Sasaki, and A. R. Burns, *Tribol. Lett.* **7**, 79 (1999).
- ¹⁸E. Cooper and G. J. Leggett, *Langmuir* **15**, 1024 (1999).
- ¹⁹J. D. Kiely and J. E. Houston, *Langmuir* **15**, 4513 (1999).
- ²⁰H. I. Kim, M. Groupe, O. Oloba, T. Doini, S. Imaduddin, T. R. Lee, and S. S. Perry, *Langmuir* **15**, 3179 (1999).
- ²¹M. D. Mowery, S. Kopta, D. F. Ogletree, M. Salmeron, and C. E. Evans, *Langmuir* **15**, 5118 (1999).
- ²²S.-S. Wong, H. Takano, and M. D. Porter, *Anal. Chem.* **70**, 5200 (1998).

- ²³R. W. Carpick and M. Salmeron, Chem. Rev. (Washington, D.C.) (Washington, D.C.) **97**, 1163 (1997), and references therein.
- ²⁴M. Garcia-Parajo, C. Longo, J. Servat, P. Gorostiza, and F. Sanz, Langmuir **13**, 2333 (1997).
- ²⁵H. I. Kim, T. Koini, T. R. Lee, and S. S. Perry, Langmuir **13**, 7192 (1997).
- ²⁶A. Lio, D. H. Charych, and M. Salmeron, J. Phys. Chem. B **101**, 3800 (1997).
- ²⁷A. Lio, C. Morant, D. Ogletree, and M. Salmeron, J. Phys. Chem. B **101**, 4767 (1997).
- ²⁸M. T. McDermott, J.-B. D. Green, and M. D. Porter, Langmuir **13**, 2504 (1997).
- ²⁹Y. Liu, D. F. Evans, Q. Song, and D. W. Grainger, Langmuir **12**, 1235 (1996).
- ³⁰X. Xiao, J. Hu, D. H. Charych, and M. Salmeron, Langmuir **12**, 235 (1996).
- ³¹J. A. Harrison, G. T. Gao, R. J. Harrison, G. M. Chateaufneuf, and P. T. Mikulski, *Encyclopedia of Nanoscience and Nanotechnology*, edited by H. S. Nalwa (American Scientific, Los Angeles, CA, 2004), pp. 511–527.
- ³²B. Park, M. Chandross, M. J. Stevens, and G. S. Grest, Langmuir **19**, 9239 (2003).
- ³³M. Chandross, G. S. Grest, and M. J. Stevens, Langmuir **18**, 8392 (2002).
- ³⁴Y. Leng and S. Jiang, J. Am. Chem. Soc. **124**, 11764 (2002).
- ³⁵P. T. Mikulski and J. A. Harrison, J. Am. Chem. Soc. **123**, 6873 (2001).
- ³⁶P. T. Mikulski and J. A. Harrison, Tribol. Lett. **10**, 29 (2001).
- ³⁷Y. Leng and S. Jiang, Phys. Rev. B **64**, 115415 (2001).
- ³⁸Y. Leng and S. Jiang, Phys. Rev. B **63**, 193406 (2001).
- ³⁹Y. Leng and S. Jiang, Tribol. Lett. **11**, 111 (2001).
- ⁴⁰Y. Leng and S. Jiang, J. Chem. Phys. **113**, 8800 (2000).
- ⁴¹A. B. Tutein, S. J. Stuart, and J. A. Harrison, Langmuir **16**, 291 (2000).
- ⁴²T. Ohzono and M. Fujihira, Phys. Rev. B **62**, 17055 (2000).
- ⁴³T. Ohzono, J. N. Glosli, and M. Fujihira, Jpn. J. Appl. Phys. **38**, L675 (1999).
- ⁴⁴M. Fujihira and T. Ohzono, Jpn. J. Appl. Phys. **38**, 3918 (1999).
- ⁴⁵H. Tamura, M. Yoshida, K. Kusakabe *et al.*, Langmuir **15**, 7816 (1999).
- ⁴⁶T. Ohzono, J. N. Glosli, and M. Fujihira, Jpn. J. Appl. Phys., Part 1 **37**, 6535 (1998).
- ⁴⁷T. Bonner and A. Baratoff, Surf. Sci. **377–379**, 1082 (1997).
- ⁴⁸A. Koike and M. Yoneya, Langmuir **13**, 1718 (1997).
- ⁴⁹A. Koike and M. Yoneya, J. Chem. Phys. **105**, 6060 (1996).
- ⁵⁰K. J. Tupper, R. J. Colton, and D. W. Brenner, Langmuir **10**, 2041 (1994).
- ⁵¹K. J. Tupper and D. W. Brenner, Langmuir **10**, 2335 (1994).
- ⁵²J. N. Glosli and G. M. McClelland, Phys. Rev. Lett. **70**, 1960 (1993).
- ⁵³J. A. Harrison, P. T. Mikulski, S. J. Stuart, and A. B. Tutein, *Nanotribology: Critical Assessment and Research Needs*, edited by S. M. Hsu and Z. C. Ying (Kluwer Academic, Norwell, MA, 2000), pp. 55–62.
- ⁵⁴J. A. Harrison, S. J. Stuart, and A. B. Tutein, *Interfacial Properties on the Submicron Scale* (American Chemical Society, Washington, DC, 2000).
- ⁵⁵A. B. Tutein, S. J. Stuart, and J. A. Harrison, J. Phys. Chem. B **103**, 11357 (1999).
- ⁵⁶S. J. Stuart, A. B. Tutein, and J. A. Harrison, J. Chem. Phys. **112**, 6472 (2000).
- ⁵⁷D. W. Brenner, Phys. Rev. B **42**, 9458 (1990).
- ⁵⁸D. W. Brenner, O. A. Shenderova, J. A. Harrison, S. J. Stuart, B. Ni, and S. B. Sinnott, J. Phys.: Condens. Matter **14**, 783 (2002).
- ⁵⁹D. W. Brenner, J. A. Harrison, R. J. Colton, and C. T. White, Thin Solid Films **206**, 220 (1991).
- ⁶⁰R. W. Carpick (private communication).
- ⁶¹J. N. Glosli and F. H. Ree, Phys. Rev. Lett. **82**, 4659 (1999).
- ⁶²G. T. Gao, P. T. Mikulski, and J. A. Harrison, J. Am. Chem. Soc. **124**, 7202 (2002).
- ⁶³N. A. Marks, N. C. Cooper, and D. R. McKenzie, Phys. Rev. B **65**, 075411 (2002).
- ⁶⁴G. T. Gao, P. T. Mikulski, G. M. Chateaufneuf, and J. A. Harrison, J. Phys. Chem. B **107**, 11082 (2003).
- ⁶⁵S. B. Sinnott, R. J. Colton, C. T. White, O. A. Shenderova, D. W. Brenner, and J. A. Harrison, J. Vac. Sci. Technol. A **15**, 936 (1997).
- ⁶⁶N. A. Marks, D. R. McKenzie, B. A. Pailthorpe, M. Bernasconi, and M. Parrinello, Phys. Rev. Lett. **76**, 768 (1996).
- ⁶⁷M. M. M. Bilek, D. R. McKenzie, D. G. McCulloch, and C. M. Goringe, Phys. Rev. B **62**, 3071 (2000).
- ⁶⁸D. G. McCulloch, D. R. McKenzie, and C. M. Goringe, Phys. Rev. B **61**, 2349 (2000).
- ⁶⁹H. Jager and K. Albe, J. Appl. Phys. **88**, 1129 (2000).
- ⁷⁰I. I. Olenik, D. G. Pettifor, A. P. Sutton, and J. E. Butler, Diamond Relat. Mater. **9**, 241 (2000).
- ⁷¹H.-P. Kaukonen and R. M. Nieminen, Phys. Rev. Lett. **68**, 620 (1992).
- ⁷²A. Erdemir and C. Donnet, *Modern Tribology Handbook* (CRC, Boca Raton, FL, 2001), pp. 871–908, and references therein.
- ⁷³J. A. Heimberg, K. J. Wahl, I. L. Singer, and A. Erdemir, Appl. Phys. Lett. **78**, 2449 (2001).
- ⁷⁴M. D. Perry and J. A. Harrison, J. Phys. Chem. **99**, 9960 (1995).
- ⁷⁵P. van der Ploeg and H. J. C. Berendsen, J. Chem. Phys. **76**, 3271 (1982).
- ⁷⁶H. J. C. Berendsen, J. P. M. Postma, W. F. van Gunsteren, A. DiNola, and J. Haak, J. Chem. Phys. **81**, 3684 (1984).
- ⁷⁷K. Kojio, A. Takahara, and T. Kajiyama, Langmuir **14**, 971 (1998).
- ⁷⁸G. Y. Liu and M. B. Salmeron, Langmuir **10**, 367 (1994).
- ⁷⁹M. T. McDermott, J.-B. D. Green, and M. D. Porter, Langmuir **13**, 2504 (1997).
- ⁸⁰Q. Zhang and L. A. Archer, J. Phys. Chem. B **107**, 13123 (2003).
- ⁸¹N. Camillone, C. E. D. Chidsey, G. Y. Liu, and G. J. Scoles, J. Chem. Phys. **94**, 8493 (1991).